Medicinal Chemistry Research
https://doi.org/10.1007/s00044-019-02374-w

MEDICINAL CHEMISTRY RESEARCH

ORIGINAL RESEARCH

Preparation and biological evaluation of quinoline amines as anticancer agents and its molecular docking

Kailasam N. Vennila[1] · Kolandhaivel Prabha[2] · Deval Sunny[3] · Subbiah Madhuri[3] · Kuppannagounder P. Elango[1]

Received: 7 February 2019 / Accepted: 22 May 2019

Abstract

A series of 2-chloro N-substituted amino quinolines (**2a–2j**) were prepared and characterized by analytical and spectroscopic methods. As quinoline is an important pharmacophoric moiety, the prepared compounds were screened against a non-small cell lung cancer cell line, A549. One of the compounds, 2-chloro-8-methyl-N-(quinolin-5-yl)quinolin-4-amine (**2b**) is found to be active with inhibition concentration value of (IC_{50}) 29.4 μM. The molecular docking studies with the predominant PI3K/AKT/mTOR pathway proteins also revealed the lesser binding energy with **2b**. All the compounds are predicted to satisfy the ADME profile and the results let us to consider **2b** as a lead compound for new generation of A549 cell line inhibitors and for further studies in this way.

Keywords Amino quinolones · Anti-proliferation · Induced fit docking · Anticancer · A549 cells

Introduction

The nitrogen containing heterocycles are important structural motifs of various bioactive compounds. The value of quinoline accounts for its basis for the biologically significant molecules with diverse therapeutic profiles (Feldman et al. 2005; Shivakumar et al. 2010; Solomon 2011; Chan et al. 2013a, b; Manohar et al. 2014; Afzal et al. 2015; Bispo et al. 2015). 4-Aminoquinoline based compounds are known for their antimalarial (O'Neill et al. 2006; Eswaran et al. 2010; Sáenz et al. 2012; Rudrapal et al. 2013; O'Brien et al. 2014a), antimicrobial (Bhat et al. 2013; Rudrapal et al. 2013), anticancer activities (Eswaran et al. 2010; Thomas et al. 2011; Ren et al. 2013; Manohar et al. 2014; Verbanac et al. 2016; Mandewale et al. 2017; Rabal et al. 2018) etc. Recently, a series of 2-styryl-4-aminoquinoline was developed with potent in vitro antiproliferative activity against lung, colon, and liver cancer cell lines (El-Sayed et al. 2018). Ghorab et al. (2014) have reported a series of 4-aminoquinoline derivatives showing remarkable cytotoxicity values when compared to doxorubicin in MCF-7 cell lines. Bosutunib, neratnib and pelitinib are few of the quinoline containing anticancer drugs in the literature inhibiting different target proteins. The results of structure–activity relationship studies have shown that the anticancer activity of quinoline scaffold was found to be dependent on the position of the substituents (Shaikh et al. 2017; Rabal et al. 2018). Thus, developing a novel cytotoxic drug using this scaffold with potent activity and selectivity still remains as an interesting field of research.

Literature survey has revealed that PI3K/AKT/mTOR is the most common signaling pathway that plays a role in multiple cancers by apoptosis and cell proliferation (Bai et al. 2016; Kawade 2018; Zhao et al. 2018). Earlier reports have also revealed that A549 adenocarcinoma cells are more prone to PI3K/AKT/mTOR inhibitors (Korrodi-Gregório et al. 2016; Fang et al. 2017). The multitargeted approach is gaining attention due to the fact that inhibition of the targets in a particular pathway will be meaningful and pharmacologically significant especially in diseases such as cancer and diabetes (Singh and Bast 2014; Rehan and Bajouh 2018).

Supplementary information The online version of this article (https://doi.org/10.1007/s00044-019-02374-w) contains supplementary material, which is available to authorized users.

✉ Kuppannagounder P. Elango
drkpelango@rediffmail.com

[1] Department of Chemistry, Gandhigram Rural Institute (Deemed to be University), Gandhigram 624302, India

[2] Department of Chemistry, K. S. Rangasamy College of Technology, Tiruchengodu 637211, India

[3] National Institute of Animal Biotechnology, Hyderabad 500049, India

Published online: 01 June 2019

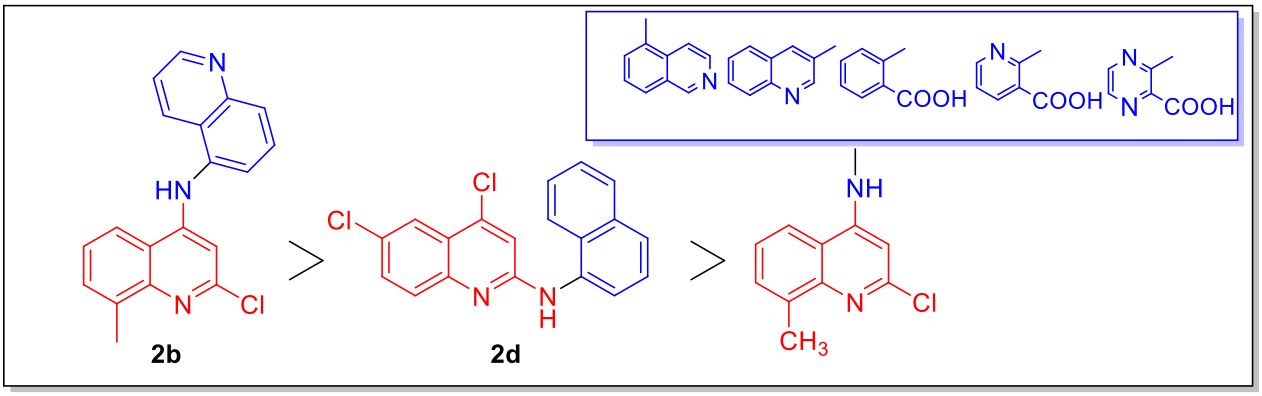

Scheme 1 The effect of structure on the efficacy of antiproliferative behavior

Though PI3K/AKT/mTOR pathway is a crucial regulatory system, 3-phosphoinositide dependent kinase-1 (PDK1), which activates the central kinase in this pathway by the phosphorylation of AKT, is an emerging drug target (Mora et al. 2004). The inhibition of this tyrosine kinase is affected by blocking it at ATP binding site (Sestito et al. 2015). Many scaffolds are reported to fit in the hinge region of the ATP binding site of PDK1 which includes dibenzo naphthrydines (Gopalsamy et al. 2007), azaindoles, aminoindazoles (Medina et al. 2010), oxindoles, pyrrolo pyrimidines (Murphy et al. 2011; O'Brien et al. 2014b, a), imidazo, anilino quinolones (O'Brien et al. 2014a), etc. NMR spectroscopy fragment screening of PDK1 afforded a quinoline analog with greater than five-fold selectivity against other key pathway kinases (Johnson et al. 2011). All these facts motivated us to focus on 2-chloro-NH substituted quinoline amines which are anticipated to be as potent as structurally related quinolines. The cytotoxic activity of the compounds was evaluated in A549, a non-small cell lung cancer cell line. Further, the literature reports on over expression of PDK1 in lung and breast cancer cells intuitively made us to focus on the quinolines for its inhibition. The main objective, therefore, of the present endeavor is to carry out molecular docking study of these compounds to describe the binding possibility and pattern of the ligands into the receptor pocket of PI3K/AKT/mTOR pathway proteins and the drug likeliness (ADME/Tox) profiling. The compounds were also screened against a non-small cell lung cancer A549 cell lines.

Results and discussion

Ten 4-subsitituted amino quinolines (**2a–j**) were prepared as shown in Scheme 1 (Prabha and Prasad 2014). All the compounds were purified by column chromatography and were characterized by spectral and analytical techniques. Anticancer activity of these compounds was screened against A549 cell line using MTT [(3-[4,5-methylthiazol-2-yl]-2,5-diphenyl-tetrazolium bromide)] assay. Molecular docking studies were also carried out to substantiate the mode of interaction of these compounds with multi targets involved in cancer cell signaling pathways.

Biological evaluation

The antiproliferative activity of these compounds was screened against the non-small cell lung cancer cell line, A549. Pemetrexed, a marketed lung cancer drug was used as a reference. Though mechanism of action of the title compounds in cells might be different from the pemetrexed, this cytotoxicity study serves as the initial biological screening. Preclinical studies have suggested that the pemetrexed has more promising activity in non-small lung cancer cell lines (Chattopadhyay et al. 2007; Joerger et al. 2010). Also, the recent study by Fang et al. (2017) have identified the enrichment of PI3K/AKT pathway in differential expression in A549 cells and the sequence of events in the pathway starts by activation of PDK1. From human protein atlas (www.proteinatlas.org), it is inferred that the PDK1 expression in lung cancer cell lines is the highest one among various cell lines. Hence, the most commonly studied lung cancer cell line A549 was used in examining the antiproliferative effects of the compounds.

MTT assay was used to detect the inhibition concentration of the compounds and the results were interpreted in terms of IC_{50} values. The percentage of cell viability was measured by determining the OD values for various concentrations ranging from 10^{-8} to 1 mM. Three of the compounds showed cytotoxic effect to cancer cells in less micromolar concentrations. To be specific, **2b** significantly affects the cells with IC_{50} value of 29.4 μM which is comparable in activity with the positive control, pemetrexed (IC_{50} 1.15 μM) (Fig. 1). The antiproliferative behavior of **2d**

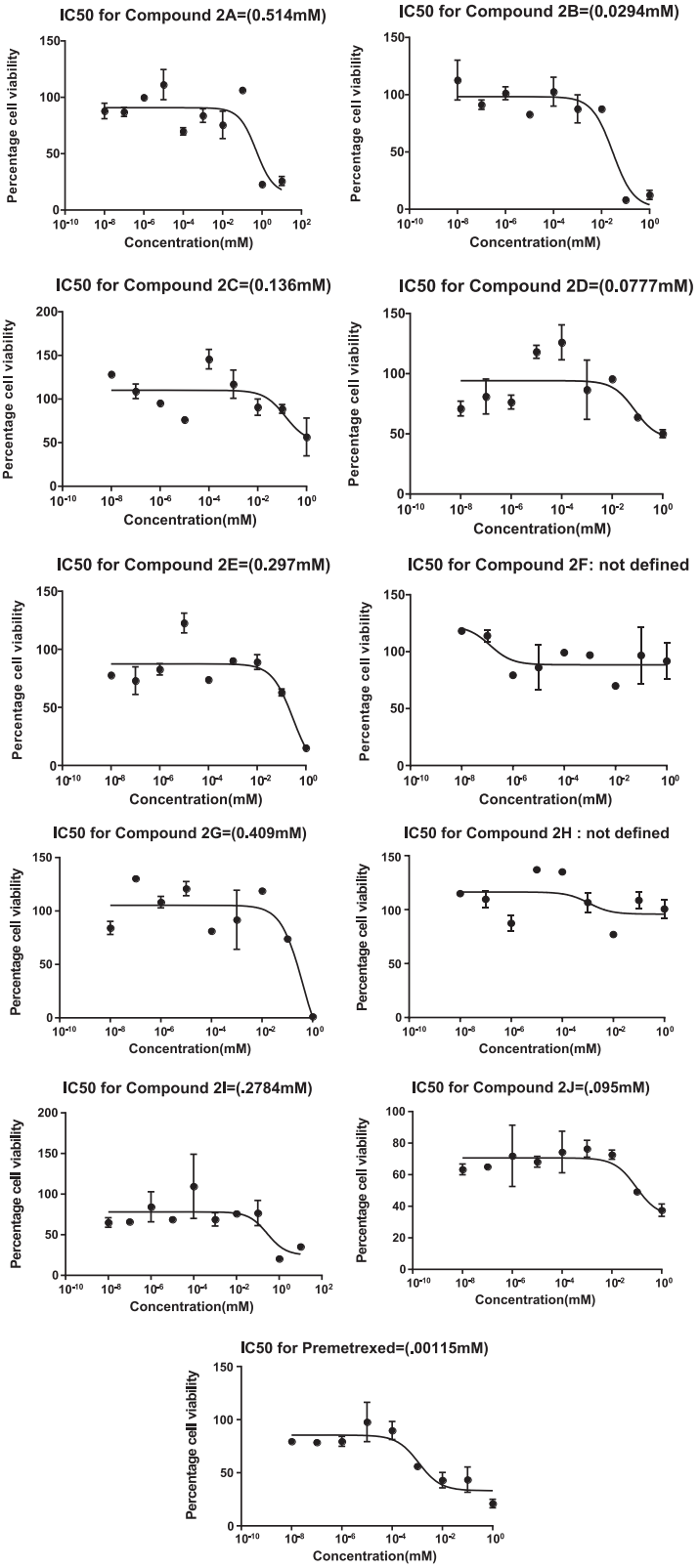

Fig. 1 A549 Cell viability percentage against various concentrations of the test compounds and their IC_{50} values by MTT assay

(IC_{50} 77.7 μM) is also found to be good. The hydrophobic methyl group at 8-position and the high electron withdrawing chloro substituent or the presence of bulky group at 2-position of quinoline ring might be attributed to the higher activity of the compound (Scheme 2). It is worth noting that the pyrazine and quinoline carboxylic acid derivatives were

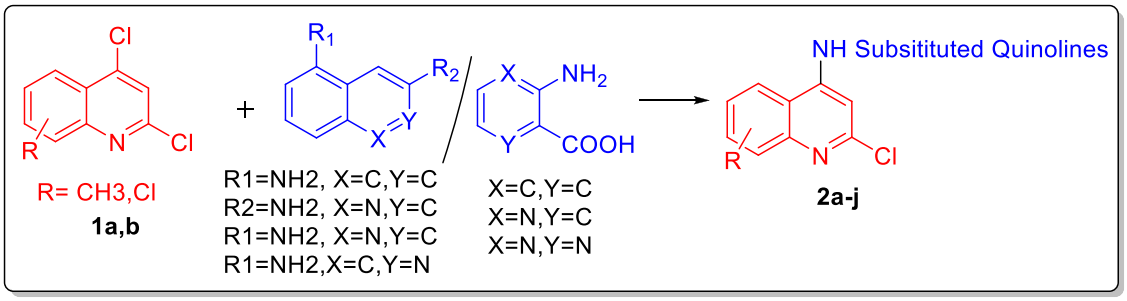

Scheme 2 Preparation of the compounds

found in ATP site inhibition of other kinases (Forns et al. 2012; Oyallon et al. 2018). Also from Fig. 1, it can be noted that the IC_{50} value could not be defined at the mentioned concentration range for the compounds **2f** and **2h**, which might be difficult to test at higher concentrations because of issues with solubility of the compounds. Thus, the activity profile displayed that the compound **2b** served best among the test compounds and can be further taken for designing a lead compound to act as A549 cancer cell line inhibitors.

Docking study

Recent years have seen an explosion in number of PI3K/AKT/mTOR pathway inhibitors which are under clinical investigations (Dienstmann et al. 2014). However due to multiple side effects, off target effects and questionable efficacies, the multitarget approaching is gaining importance. In order to elucidate the binding mode with the four major proteins involved in PI3K cell signaling pathway, we performed induced fit molecular docking studies with the compounds under investigation. The IFD docking results with glide scores, glide energy and the hydrogen bonded residues with each of the proteins are given in Table 1 and the interactions are shown in Fig. 2 and Fig. S1.

The docking results indicated that the experimentally well performed compound **2b** came out in top three with the good G-scores (−10.12, −7.9, −9.971, and −9.824 kcal/mol) and glide energy (−49.989, −50.164, −53.661, and −51.673 kJ/mol) with the targets PI3K, PDK1, AKT, and mTOR, respectively. In PI3K, though the compound **2b** in sixth position, the glide energy values did not differ much and high glide score as well with respect to the third compound **2j**. Each of the compound's binding behavior is found to be different for all the four protein molecules. Though **2f** was found to be with greater energy scores with PDK1 and AKT, it is not in PI3K1 and mTOR. Docking score wise sorting of compounds revealed that the better forming protein ligand complexes are PI3K-**2f**, PDK1-**2a**, AKT-**2f**, and mTOR-**2c**. From these results, both the glide score and glide energy with respect to all the four major proteins is found to be good for **2b** and its interactions in the binding sites of all the four proteins were given in Fig. 2. In **2b**, the presence of a highly electronegative chlorine substituent and the methyl group made the quinoline system to flip in such a way to fit in the hydrophobic space of the active site. Hence, the occupancy of the hydrophobic space by quinoline moiety in the hinge region of ATP site in PDK1 and strong interactions with key residues together will lead to a better inhibitor. Though, the docking results and antiproliferative cell line screening cannot be related directly due to the nonavailability of mechanism of action of compounds in the cells, this study can serve as a preliminary basis for further designing inhibitors for this pathway. Thus, the compound **2b** in this case is found to perform better both in cell line screening and computational studies and it will serve as a good start for optimization to further develop potent PI3K/PDK/AKT/mTOR inhibitors. However the cell line toxicity might be associated with other cellular mechanisms for the test compounds and these

Table 1 IFD results of the title compounds

Protein	Compounds	*G*-score (kcal/mol)	Glide energy (kJ/mol)
PI3K	2h	−7.173	−55.98
	2f	−2.062	−54.061
	2j	−3.167	−52.363
	2g	−7.178	−50.943
	2e	−10.059	−50.832
	2b	**−10.12**	**−49.989**
PDK-1	2d	−6.249	−64.603
	2b	**−7.91**	**−50.164**
	2f	−6.521	−50.651
AKT1	2f	−11.445	−56.127
	2b	**−9.971**	**−53.661**
	2h	−7.746	−53.563
mTOR	**2b**	**−9.824**	**−51.673**
	2i	−10.285	−51.259
	2j	−6.457	−50.692

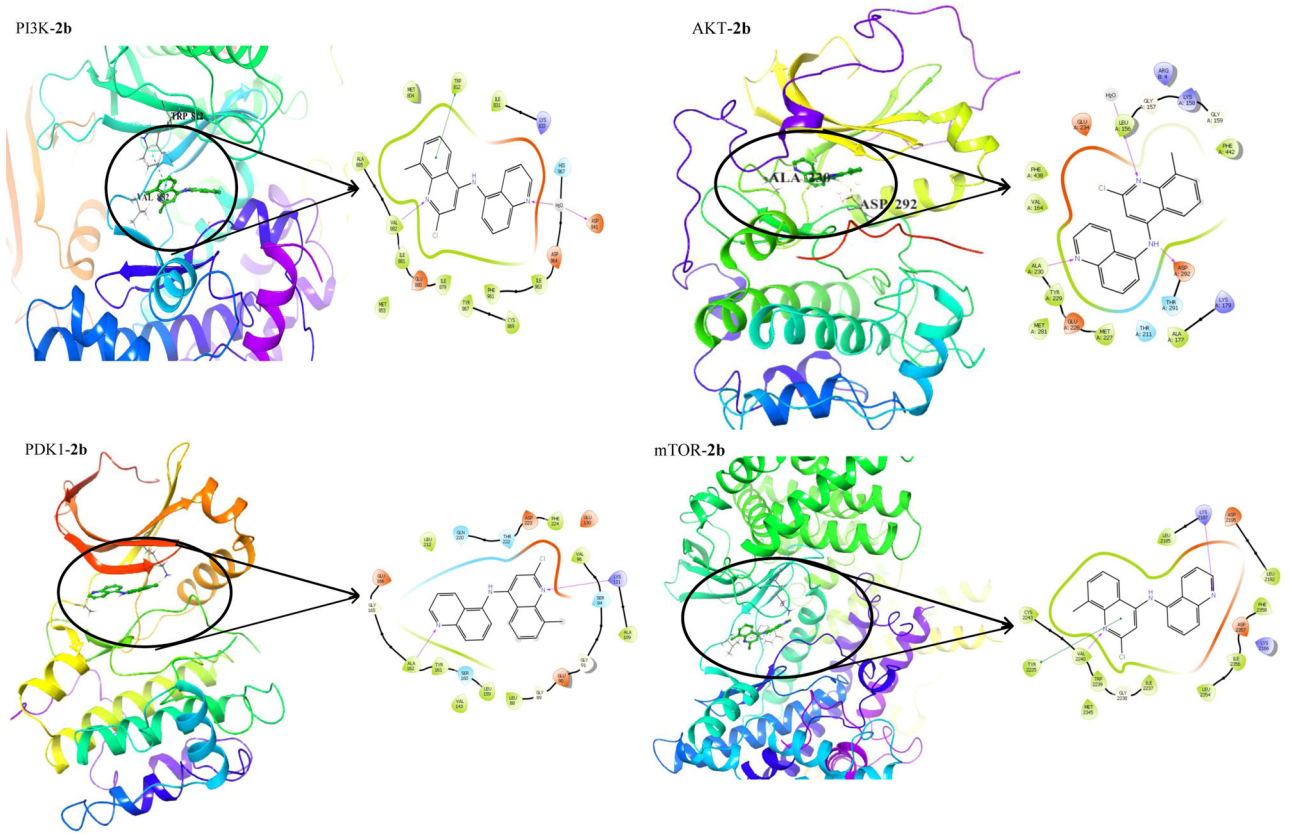

Fig. 2 Binding site interactions of **2b** with PI3K (PDB Id: 3l54), PDK1 (PDB Id: 2r7b), AKT (PDB ID: 3mvh), and mTOR (PDB ID: 4jt6)

preliminary docking results supports the proposed inhibition of PI3K/PDK/AKT/mTOR pathway.

ADME profile

The fast and the trustworthy predictions of pharmacological profiles such as adsorption, distribution, metabolism, and excretion properties will always lead to the successful drug discovery. Hence, the ADME properties along with important topological descriptors of the test compounds were predicted using molecular descriptor wizard by Qikprop in Maestro (Schrödinger Release 2018-2: QikProp, Schrödinger, LLC, New York, NY). According to the Lipinski's rule, molecules with good membrane permeability have log $P \leq 5$, molecular weight ≤500, number of hydrogen bond acceptors ≤10, and number of hydrogen bond donors ≤5 (De La Nuez and Rodríguez 2008; Mondal et al. 2009; Yasmin et al. 2017). The active compound **2b** has about 100% human oral absorption and satisfied Lipinski rule of five. log $P_{o/w}$ (octanol/water coefficient), log K_{hsa} (human serum albumin binding), log BB (blood brain barrier penetration), log h_{ERG} (ion channel inhibition), and log K_p (skin permeability) were found to be in normal ranges(Singh and Bast 2014) (Table S1).

Conclusion

We have prepared a series of N-substituted 4-aminoquinoline analogs (**2a–j**) with modification of ring systems and the substitutions of the attached amines. The antiproliferative screening results revealed that the compound **2b** is the most active agent against A549, a nonsmall cell lung cancer cell lines with IC_{50} of 29.4 µM. Moreover, the docking calculations showed that the compound **2b** binds efficiently by strong interactions with key residues of four critical proteins in PI3K/AKT/mTOR pathway with lesser binding energy. Compound **2b** performed better both in biological and computational studies with satisfactory ADME profile and it will serve as a good start to generate more potent PDK1 inhibitors.

Experimental

Preparation of quinoline amines

2-Chloro-NH substituted quinoline amines were prepared as described, by one of the co-authors, in literature (Vennila et al. 2010; Prabha and Prasad 2014). In a typical

Table 2 Synthesis and reaction conditions of compound **2a–j**

Comp d.	Amines	Products	t (h)	T (°C)	Compds	Amines	Products	t (h)	T (°C)
2a	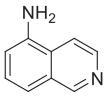	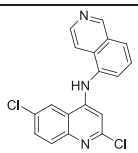	0.5	180	**2f**	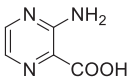	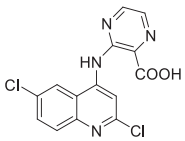	0.5	140
2b		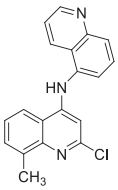	0.5	180	**2g**	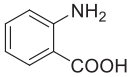	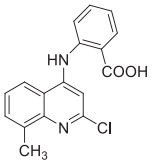	0.5	120
2c	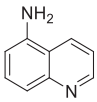	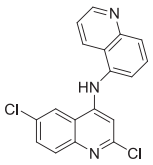	0.5	180	**2h**	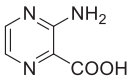	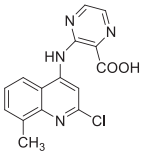	0.5	140
2d	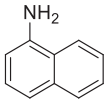	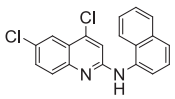	0.5	110	**2i**	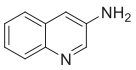	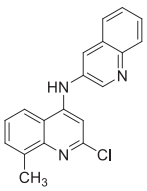	0.5	190
2e	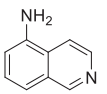	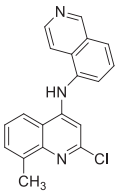	0.5	180	**2j**	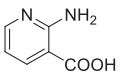	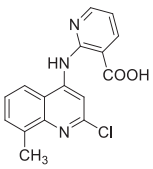	0.5	140

experiment, an equimolar mixture of 8-methyl or 6-chloro quinoline (0.01 mol) and varieties of aminoquinoline/aminocarboxylic acids (0.01 mol) was heated under neat condition. The reaction was monitored by TLC. The product obtained was washed with water, dried and purified by silica gel column chromatography ethylacetate:methanol (99:1) as an eluent to get the respective 4-amino substituted products which was recrystallized using ethanol (Scheme 2). The reaction temperature and time are collected in Table 2. The prepared compounds were characterized by elemental analysis, IR, ^{1}H NMR and mass studies (Fig. S2). The results obtained are accordance with those reported earlier.

2,6-Dichloro-N-(isoquinolin-5-yl)quinolin-4-amine (2a)

Pale brown solid; mp: 148–150 °C; Yield : (25%): IR (KBr, cm^{-1}) ν_{max}: 3290 (N-H), 1630, 1577 (C = N); ^{1}H NMR (DMSO-d_6), (ppm) δ_H: 6.64 (s, 1H, C3-H), 7.17–7.27 (m, 2H, C6', C7'-H), 7.51 (d, 1H, C8'-H, J = 8.00 Hz), 7.66 (d, 1H, C8-H, J = 7.20 Hz), 7.71 (d, 1H, C7-H, J = 8.00 Hz), 7.80 (d,1H, C4'-H, J = 7.20 Hz), 8.12 (d, 1H, C5-H, Jm = 2.00 Hz), 8.45 (d, 1H, C3'-H, J = 8.00 Hz), 8.56 (s, 1H, C1'-H), 10.10 (b s, 1H, C4-NH amino form) 12.01 (b s, 1H, N1-H imino form). The ratio of amino and imino form was found to be 1:1; LCMS m/z: $[M+H]^+$ calculated for $C_{18}H_{11}C_{l2}N_3$: 339.0, found: 340.0, Anal. Calcd. for

$C_{18}H_{11}Cl_2N_3$ (339): C, 63.55; H, 3.26; N, 12.35%; Found: C, 63.50; H, 3.30; N, 12.33%.

2-Chloro-8-methyl-N-(quinolin-5-yl)quinolin-4-amine (2b)

Brown solid; mp: 151–153 °C; Yield: (30%); IR ν_{max} (KBr, cm^{-1}): 3182 (N-H), 1625, 1594 (C = N); ^{1}H NMR (DMSO-d_6), (ppm) δ_H: 2.72 (s, 3H, C8-CH_3), 6.73 (s, 1H, C3-H), 7.35 (d, 1H, C8'-H J = 8.50 Hz), 7.51 (d, 1H, C6-H J = 7.00 Hz), 7.60–7.80 (m, 4H, C7, C7', C4' and C3'-H), 8.11 (d, 1H, C6'-H J = 7.00 Hz), 8.29 (d, 1H, C5-H J = 8.50 Hz), 8.80 (d, 1 H, C2'-H J = 9.00 Hz), 11.50 (b s, 1H, C4-NH amino form); 12.55 (bs, 1H, C_1-NH imino form, ratio of amino form : imino form is 1 : 1), Anal. Calcd. for $C_{19}H_{14}ClN_3$ (319): C, 71.36; H, 4.41; N, 13.14%; Found: C, 71.34; H, 4.38; N, 13.11%.

2,6-Dichloro-N-(quinolin-5-yl)quinolin-4-amine (2c)

Brown solid; mp: 149–151 °C; Yield : (30%); IR ν_{max} (KBr, cm^{-1}): 3180 (N-H), 1627, 1598 (C = N); ^{1}H NMR (DMSO-d_6) (ppm) δ_H: 6.71 (s, 1H, C3-H), 7.34 (d, 1H, C8'-H J = 8.50 Hz), 7.58 (d, 1H, C8-H J = 8.50 Hz), 7.63-7.99 (m, 4H, C7, C7', C4' and C3'-H), 8.15 (d, 1H, C6'-H J = 7.00 Hz), 8.30 (s, 1H, C5-H), 8.90 (d, 1H, C2'-H J = 9.00 Hz), 11.87 (b s, 1H, C4-NH amino form); 12.80 (bs, 1H, C_1-NH imino form, ratio of amino form : imino form is 1 : 1), Anal. Calcd. for $C_{18}H_{11}C_{12}N_3$ (339): C, 63.55; H, 3.26; N, 12.35%; Found: C, 63.51; H, 3.20; N, 12.33%.

4,6-Dichloro-N-(naphthalen-1-yl)quinolin-2-amine (2d)

Pale yellow spongy mass; mp: 116–118 °C; Yield: (43%); IR (KBr, cm^{-1}) ν_{max}: 3120 (N-H), 1597 (C = N); ^{1}H NMR ($CDCl_3$) (ppm) δ_H: δ 6.91 (s, 1H, C_3-H), 7.21 (s, 1H, C_2-NH), 7.50–7.94 (m, 8H, C_7, C_2'- C_8'-H), 8.00 (d, 1H, C_5-H J_m = 2.40 Hz), 8.04 (d, 1H, C_8-H J = 8.00 Hz); Anal. Calcd for $C_{19}H_{12}Cl_2N_2$ (338): C, 67.27; H, 3.57; N, 8.26%; Found: C, 67.13; H, 3.55; N, 8.23%.

2-Chloro-N-(isoquinolin-5-yl)-8-methylquinolin-4-amine (2e)

Pale brown solid; mp: 145–147 °C; Yield: (30%); IR ν_{max} (KBr, cm^{-1}): 3200 (N-H), 1608, 1566 (C = N); ^{1}H NMR (DMSO-d_6) (ppm) δ_H: 2.74 (s, 3H, C8-CH_3), 6.60 (s, 1H, C3-H), 7.20–7.31 (m, 2H, C6', C7'-H), 7.59 (t, 1H, C6-H, J = 7.60 Hz), 7.65 (d, 1H, C8'-H, J = 8.00 Hz), 7.76 (d, 1H, C4'-H, J = 7.20 Hz), 7.85 (d, 1H, C7-H, J = 8.40 Hz), 8.21 (d, 1H, C5-H, J = 8.20 Hz), 8.50 (d, 1H, C3'-H, J = 8.00 Hz), 8.69 (s, 1H, C1'-H), 11.15 (b s, 1H, C4-NH amino form); 12.34 (bs, 1H, C_1-NH imino form, ratio of amino form : imino form is 1 : 1), LCMS m/z: $[M+H]^+$ calculated for $C_{19}H_{14}ClN_3$: 319.0, found: 319.0.Anal. Calcd. for $C_{19}H_{14}ClN_3$ (319): C, 71.36; H, 4.41; N, 13.14%; Found: C, 71.29; H, 4.40; N, 13.12%.

3-(2,6-Dichloroquinolin-4-ylamino)pyrazine-2-carboxylic acid (2f)

Pale green solid; mp: 162–164 °C; Yield: (32%); IR (KBr, cm^{-1}) ν_{max}: 3450 (O-H), 3296 (N-H), 1711 (C = O), 1643, 1548 (C = N); ^{1}H NMR (DMSO-d_6) (ppm) δ_H: 6.80 (s, 1H, C_3-H), 7.65 (d, 1H, C8-H J = 8.50 Hz), 7.77 (d, 1H, C_7-H J = 9.00 Hz), 7.99 (s, 1H, C_5-H), 8.30 (d, 1H, C_5'-H J = 5.00 Hz), 8.49 (d, 1H, C_6'-H J = 5.50 Hz), 10.24 (bs, 1H, C_4-NH amino form), 12.62 (bs, 1H, C_1-NH imino form, ratio of amino form : imino form is 1 : 1), 14.25 (bs, 1H, C_3'-OH); Anal. Calcd. for $C_{14}H_8Cl_2N_4O_2$ (334): C, 50.17; H, 2.41; N, 16.72%; Found: C, 50.12; H, 2.40; N, 16.69;%.

2-(2-Chloro-8-methylquinolin-4-ylamino) benzoic acid (2g)

Pale greenish yellow solid; mp: 140–142 °C; Yield: (30%); IR (KBr, cm^{-1}) ν_{max}: 3445 (O-H), 3290 (N-H), 1749 (C = O), 1621(C = N); ^{1}H NMR (DMSO-d_6) (ppm) δ_H: 2.94 (s, 3H, C_8-CH_3), 6.41 (s, 1H, C_3-H), 7.36–7.70 (m, 5H, C_3'-C_6', C_6-H), 7.79 (d, 1H, C_7 -H J = 8.40 Hz), 8.33 (d, 1H, C_5-H J = 7.60 Hz), 11.42 (bs, 1H, C_4-NH amino form), 12.53 (bs, 1H, C_1-NH imino form, ratio of amino form : imino form is 1 : 1), 14.10 (bs, 1H, C_1'-OH); MSEI m/z 312 (M^+, 42), 314 (M+2, 13), Anal. Calcd. for $C_{17}H_{13}ClN_2O_2$ (312): C, 65.29; H, 4.19; N, 8.96; %; Found: C, 65.27; H 4.17; N, 8.94%.

3-(2-Chloro-8-methylquinolin-4-ylamino)pyrazine-2-carboxylic acid (2h)

Yellow solid; mp: 158–160 °C; Yield: (29%); IR (KBr, cm^{-1}) ν_{max}: 3360 (O-H), 3155 (N-H), 1690 (C = O), 1630, 1535 (C = N); ^{1}H NMR (DMSO-d_6) (ppm) δ_H: 2.89 (s, 3H, C_8-CH_3), 6.80 (s, 1H, C_3-H), 7.52 (t, 1H, C_6-H J = 8.50 Hz), 7.62 (d, 1H, C_7-H J = 9.00 Hz), 7.68 (dd, 1H, C_5-H J = 8.00 Hz, J = 1.50 Hz), 8.22 (d, 1H, C_5'-H J = 5.50 Hz), 8.44 (d, 1H, C_6'-H J = 5.50 Hz), 10.11 (bs, 1H, C_4-NH amino form), 11.14 (bs, 1H, C_1-NH imino form, ratio of amino form : imino form is 1 : 1), 12.33 (bs, 1H, C_3'-OH); Anal. Calcd. for $C_{15}H_{11}ClN_4O_2$ (314): C, 57.24; H, 3.52; N, 17.80; Found: C, 57.23; H 3.50; N, 17.78%.

N-(2-Chloro-8-methylquinolin-4-yl)quinolin-3-amine (2i)

Brown solid; mp: 145–147 °C; Yield : (30%); IR ν_{max} (KBr, cm^{-1}): 3178 (N-H), 1629, 1590 (C = N); ^{1}H NMR (DMSO-d_6) (ppm) δH: 2.79 (s, 3H, C8-CH_3),6.73 (s, 1H, C3-H), 7.20-7.88 (m, H, C6,C5'- C8'-H), 7.93 (d, 1H, C7-H, J =

8.40 Hz), 8.33 (d, 1H, C5-H, J = 8.20 Hz), 8.70 (s, 1H, C4'-H), 9.01 (s, 1H, C1'-H), 11.11 (b s, 1H, C4-NH amino form); 12.00 (bs, 1H, C_1-NH imino form, ratio of amino form : imino form is 1:1); LCMS m/z: $[M+H]^+$ calculated for $C_{19}H_{14}ClN_3$: 319.0, found: 320.3. Anal. Calcd. for $C_{19}H_{14}ClN_3$ (319): C, 71.36; H, 4.41; N, 13.14%; Found: C, 71.34; H, 4.38; N, 13.11%.

2-(2-Chloro-8-methylquinolin-4-ylamino)nicotinic acid (2j)

Pale green solid; mp: 150–152 °C; Yield: (39%); IR (KBr, cm^{-1}) ν_{max}: 3452 (O-H), 3296 (N-H), 1715 (C = O), 1654, 1550 (C = N); ^{1}H NMR (DMSO-d_6) (ppm) δ_H: 2.86 (s, 3H, C_8-CH_3), 6.47 (s, 1H, C_3-H), 7.29 (t, 1H, C_5'-H $J = 4.80$ Hz, $J = 7.20$ Hz), 7.47 (t, 1H, C_6 -H $J = 8.40$ Hz), 7.59 (d, 1H, C_7-CH_3 $J = 8.00$ Hz), 7.79 (d, 1H, C_4'-H $J = 7.20$ Hz), 8.12 (dd, 1H, C_5-H $J = 8.80$ Hz, $J = 1.6$ Hz), 8.24(dd, 1H, C_6'-H $J = 5.60$ Hz, $J = 1.60$ Hz), 10.23 (bs, 1H, C_4-NH amino form), 12.61 (bs, 1H, C_1-NH imino form, ratio of amino form : imino form is 1:1), 14.22 (bs, 1H, C_3'-OH); Anal. Calcd. for $C_{16}H_{12}ClN_3O_2$ (313): C, 61.25; H, 3.86; N, 13.39%; Found: C, 61.19; H, 3.81; N, 13.34%.

Cytotoxic activity using MTT assay

The A549 cells (human lung carcinoma cell line) were cultured in DMEM medium supplemented with 10% fetal bovine serum (FBS) at 37 °C with 5% CO_2. The cell viability upon different compound treatments were evaluated in A549 cells by MTT (3-[4,5-methylthiazol-2-yl]-2,5-diphenyl-tetrazolium bromide) assay (D'Mello et al. 1997; Wang et al. 2014). Briefly, A549 cells (10,000 cells/well) were seeded in a 96-well plate and incubated overnight. The next day the culture medium was replaced with fresh DMEM (without FBS) and serial tenfold dilutions of the test compounds were added. Negative control wells contained only the cells without any compound, and the blank wells contained only the culture medium without cells. The cells were placed back into the incubator for next 24 h. On the day of the assay, the cells were washed with PBS gently and 100 µl of PBS was added to each well, to this 5 µl of MTT reagent (10 mg/ml) was added per well and incubated for 4 h in dark. After completing the incubation, 100 µl of 100% DMSO was added to each well and incubated in dark at room temperature for 1 h. The color developed (optical density (OD)) was measured at 570 nm. The percentage cell viability was calculated by ratio of the difference in the OD values obtained from wells carrying cells treated with compounds and the blank wells versus the difference in the OD values obtained in negative wells and the blank wells. To assess the compound's anticancer potency the IC_{50} values (the concentration that inhibited cell viability to 50% of the control) were determined using Prism version 6 (GraphPad, San Diego, CA) by nonlinear regression method.

Molecular docking

The molecular docking calculations were carried out using Glide program in Schrodinger software. The structure of the test compounds were first generated through the Maestro, a graphical interface in Schrodinger and then prepared through ligprep. The three dimensional coordinates of the four proteins were taken from Protein Data Bank with PDB IDs : 3l54, 2r7b, 3mvh, and 4jt6 were selected. Protein preparation wizard was used to prepare the protein. The missing residues were built using prime module and the structure is refined using OPLS2005 forcefield by removing the water molecules leaving the waters within 5 Å of the active site. Induced fit molecular docking calculations were performed with Glide in extra precision (XP) mode (Friesner et al. 2006) and the glide energy was used for ranking the ligands.

Acknowledgements The authors are highly thankful to the Department of Science and Technology, New Delhi for financial support under WOS-A Scheme (SR/WOS-A/CS-1084/2014). KNV acknowledges the computational facility and Schrodinger access offered by Prof. D. Velmurugan, BSR Faculty, Center for crystallography and Biophysics, University of Madras, Chennai.

Compliance with ethical standards

Conflict of interest The authors declare that they have no conflict of interest.

Ethical approval This article does not contain any studies with animals performed by any of the authors.

Informed consent Informed consent was obtained from all individual participants included in the study.

Publisher's note: Springer Nature remains neutral with regard to jurisdictional claims in published maps and institutional affiliations.

References

Afzal O, Kumar S, Haider MR et al. (2015) A review on anticancer potential of bioactive heterocycle quinoline. Eur J Med Chem 97:871–910

Bai X, Li P, Xie Y et al. (2016) Overexpression of 3-phosphoinositide-dependent protein kinase-1 is associated with prognosis of gastric carcinoma. Tumor Biol 37:2333–2339. https://doi.org/10.1007/s13277-015-4024-8

Bhat HR, Pandey PK, Ghosh SK, Singh UP (2013) Development of 4-aminoquinoline-1,3,5-triazine conjugates as potent antibacterial agent through facile synthetic route. Med Chem Res 22:5056–5065. https://doi.org/10.1007/s00044-013-0521-8

Bispo M, de LF, de Alcantara CC, de Moraes MO et al. (2015) A new and potent class of quinoline derivatives against cancer. Chem Mon 146:2041–2052. https://doi.org/10.1007/s00706-015-1570-0

Chan SH, Chui CH, Chan SW et al. (2013a) Synthesis of 8-hydroxyquinoline derivatives as novel antitumor agents. ACS Med Chem Lett 4:170–174. https://doi.org/10.1021/ml300238z

Chan SH, Chui CH, Chan SW et al. (2013b) Synthesis of 8-Hydroxyquinoline Derivatives as Novel Antitumor Agents. 4:170–174

Chattopadhyay S, Moran RG, Goldman ID (2007) Pemetrexed: biochemical and cellular pharmacology, mechanisms, and clinical applications. Mol Cancer Ther 6:404–417. https://doi.org/10.1158/1535-7163.MCT-06-0343

D'Mello SR, Borodezt K, Soltoff SP (1997) Insulin-like growth factor and potassium depolarization maintain neuronal survival by distinct pathways: possible involvement of PI 3-kinase in IGF-1 signaling. J Neurosci 17:1548–1560

De La Nuez A, Rodríguez R (2008) Current methodology for the assessment of ADME-Tox properties on drug candidate molecules. Biotecnol Apl 25:97–110

Dienstmann R, Rodon J, Serra V, Tabernero J (2014) Picking the point of inhibition: a comparative review of PI3K/AKT/mTOR pathway inhibitors. Mol Cancer Ther. https://doi.org/10.1158/1535-7163.MCT-13-0639

El-Sayed MA-A, El-Husseiny WM, Abdel-Aziz NI et al. (2018) Synthesis and biological evaluation of 2-styrylquinolines as antitumour agents and EGFR kinase inhibitors: molecular docking study. J Enzyme Inhib Med Chem 33:199–209. https://doi.org/10.1080/14756366.2017.1407926

Eswaran S, Adhikari AV, Chowdhury IH et al. (2010) New quinoline derivatives: Synthesis and investigation of antibacterial and antituberculosis properties. Eur J Med Chem 45:3374–3383. https://doi.org/10.1016/j.ejmech.2010.04.022

Fang Y, Zhang C, Wu T, et al. (2017) Transcriptome sequencing reveals key pathways and genes associated with cisplatin resistance in lung adenocarcinoma A549 cells. PLoS One 12(1):1–17. https://doi.org/10.1371/journal.pone.0170609

Feldman RI, Wu JM, Polokoff MA et al. (2005) Novel small molecule inhibitors of 3-phosphoinositide-dependent kinase-1. J Biol Chem 280:19867–19874. https://doi.org/10.1074/jbc.M501367200

Forns P, Esteve C, Taboada L et al. (2012) Pyrazine-based Syk kinase inhibitors. Bioorganic Med Chem Lett 22:2784–2788. https://doi.org/10.1016/j.bmcl.2012.02.087

Friesner RA, Murphy RB, Repasky MP et al. (2006) Extra precision glide: docking and scoring incorporating a model of hydrophobic enclosure for protein-ligand complexes. J Med Chem 49:6177–6196. https://doi.org/10.1021/jm051256o

Gopalsamy A, Shi M, Boschelli DH et al. (2007) Discovery of dibenzo[c,f][2,7]naphthyridines as potent and selective 3-phosphoinositide-dependent kinase-1 inhibitors. J Med Chem 50:5547–5549. https://doi.org/10.1021/jm070851i

Joerger M, Omlin a, Cerny T, Früh M (2010) The role of pemetrexed in advanced non small-cell lung cancer: special focus on pharmacology and mechanism of action. Curr Drug Targets 11:37–47. https://doi.org/10.2174/138945010790030974

Johnson MC, Hu Q, Lingardo L et al. (2011) Novel isoquinolone PDK1 inhibitors discovered through fragment-based lead discovery. J Comput Aided Mol Des 25:689–698. https://doi.org/10.1007/s10822-011-9456-7

Kawade VS (2018) Therapeutic Potential of PI3K/Akt/mTOR Signalling Pathway: Effective Combination Therapy for Cancer. Indian J Pharma Sci 80:702–708

Korrodi-Gregório L, Soto-Cerrato V, Vitorino R et al. (2016) From proteomic analysis to potential therapeutic targets: Functional profile of two lung cancer cell lines, A549 and SW900, widely studied in pre-clinical research. PLoS ONE 11:1–27. https://doi.org/10.1371/journal.pone.0165973

Mandewale MC, Patil UC, Shedge SV et al. (2017) A review on quinoline hydrazone derivatives as a new class of potent antitubercular and anticancer agents. Beni-Suef Univ J Basic Appl Sci 6:354–361. https://doi.org/10.1016/j.bjbas.2017.07.005

Manohar S, Pepe A, Vélez Gerena CE et al. (2014) Anticancer activity of 4-aminoquinoline-triazine based molecular hybrids. RSC Adv 4:7062–7067. https://doi.org/10.1039/c3ra45333b

Medina JR, Blackledge CW, Heerding DA et al. (2010) Aminoindazole PDK1 inhibitors: A case study in fragment-based drug discovery. ACS Med Chem Lett 1:439–442. https://doi.org/10.1021/ml100136n

Mondal SK, Mondal NB, Banerjee S, Mazumder UK (2009) Determination of drug-like properties of a novel antileishmanial compound: In vitro absorption, distribution, metabolism, and excretion studies. Indian J Pharmacol 41:176–181. https://doi.org/10.4103/0253-7613.56075

Mora A, Komander D, Van Aalten DMF, Alessi DR (2004) PDK1, the master regulator of AGC kinase signal transduction. Semin. Cell Dev. Biol. 15:161–170

Mostafa M. Ghorab, Mansour S, Al said RKA (2014) Design, synthesis and potential anti-proliferative activity of some novel 4-aminoquinoline derivatives Acta Pharm 64:285–297. https://doi.org/10.2478/acph-2014-0030

Murphy ST, Alton G, Bailey S et al. (2011) Discovery of novel, potent, and selective inhibitors of 3-phosphoinositide-dependent kinase (PDK1). J Med Chem 54:8490–8500. https://doi.org/10.1021/jm201019k

O'Brien NJ, Brzozowski M, Buskes MJ et al. (2014a) Synthesis and biological evaluation of 2-anilino-4-substituted-7H-pyrrolopyrimidines as PDK1 inhibitors. Bioorg Med Chem 22:3879–3886. https://doi.org/10.1016/j.bmc.2014.06.018

O'Brien NJ, Brzozowski M, Wilson DJD et al. (2014b) Synthesis and biological evaluation of substituted 2-anilino-7H-pyrrolopyrimidines as PDK1 inhibitors. Tetrahedron 70:4947–4956. https://doi.org/10.1016/j.tet.2014.05.033

O'Neill PM, Ward Sa, Berry NG et al. (2006) A medicinal chemistry perspective on 4-aminoquinoline antimalarial drugs. Curr Top Med Chem 6:479–507. https://doi.org/10.2174/156802606776743147

Oyallon B, Brachet-Botineau M, Logé C et al. (2018) Structure-based design of novel quinoxaline-2-carboxylic acids and analogues as Pim-1 inhibitors. Eur J Med Chem 154:101–109. https://doi.org/10.1016/j.ejmech.2018.04.056

Prabha K, Prasad KJR (2014) Synthesis and spectroscopic distinction of benzonaphthonaphthyridine and its isomer. Synth Commun 1441–1452. https://doi.org/10.1080/00397911.2013.831104

Rabal O, Sánchez-Arias JA, San José-Enériz E, et al. (2018) Detailed Exploration around 4-Aminoquinolines Chemical Space to Navigate the Lysine Methyltransferase G9a and DNA Methyltransferase (DNMT) Biological Spaces. J Med Chem https://doi.org/10.1021/acs.jmedchem.7b01925

Rehan M, Bajouh OS (2018) Virtual screening of naphthoquinone analogs for potent inhibitors against the cancer-signaling PI3K/AKT/mTOR pathway. J Cell Biol 1–12. https://doi.org/10.1002/jcb.27100

Ren J, Zhao J, Zhou Y-S et al. (2013) Synthesis and antitumor activity of novel 4-aminoquinoline derivatives. Med Chem Res 22:2855–2861. https://doi.org/10.1007/s00044-012-0283-8

Rudrapal M, Chetia D, Prakash A (2013) Synthesis, antimalarial-, and antibacterial activity evaluation of some new 4-aminoquinoline derivatives. Med Chem Res 22:3703–3711. https://doi.org/10.1007/s00044-012-0371-9

Sáenz FE, Mutka T, Udenze K et al. (2012) Novel 4-aminoquinoline analogs highly active against the blood and sexual stages of Plasmodium in vivo and in vitro. Antimicrob Agents Chemother 56:4685–4692. https://doi.org/10.1128/AAC.01061-12

Schrödinger Release 2018-2: QikProp, Schrödinger, LLC, New York, NY 2018. schrodinger.pdf

Sestito S, Nesi G, Daniele S et al. (2015) Design and synthesis of 2-oxindole based multi-targeted inhibitors of PDK1/Akt signaling pathway for the treatment of glioblastoma multiforme. Eur J Med Chem 105:274–288. https://doi.org/10.1016/j.ejmech.2015.10.020

Shaikh SKJ, Kamble RR, Somagond SM et al. (2017) Tetrazolylmethyl quinolines: design, docking studies, synthesis, anticancer and antifungal analyses. Eur J Med Chem 128:258–273. https://doi.org/10.1016/j.ejmech.2017.01.043

Shivakumar D, Williams J, Wu Y et al. (2010) Prediction of absolute solvation free energies using molecular dynamics free energy perturbation and the OPLS force field. J Chem Theory Comput 6:1509–1519. https://doi.org/10.1021/ct900587b

Singh P, Bast F (2014) Multitargeted molecular docking study of plant-derived natural products on phosphoinositide-3 kinase pathway components. Med Chem Res. https://doi.org/10.1007/s00044-013-0774-2

Thomas KD, Adhikari AV, Telkar S et al. (2011) Design, synthesis and docking studies of new quinoline-3-carbohydrazide derivatives as antitubercular agents. Eur J Med Chem 46:5283–5292. https://doi.org/10.1016/j.ejmech.2011.07.033

Solomon VR (2011) Quinoline as a privileged scaffold in drug discovery. Curr Med Chem 18:1488–1508. HL

Vennila KN, Prabha K, Manoj M, et al. (2010) 2-Chloro-7-methyl-12-phenyldibenzo[*b*, *g*][1,8]naphthyridin-11(6 *H*)-one. Acta Crystallogr Sect E Struct Reports Online 66:o1823–o1823. https://doi.org/10.1107/S160053681002430X

Verbanac D, Malik R, Chand M et al. (2016) Synthesis and evaluation of antibacterial and antioxidant activity of novel 2-phenylquinoline analogs derivatized at position 4 with aromatically substituted 4H-1,2,4-triazoles. J Enzyme Inhib Med Chem 31:104–110. https://doi.org/10.1080/14756366.2016.1190714

Wang J, Li J, Lu A, et al. (2014) Anticancer effect of salidroside on A549 lung cancer cells through inhibition of oxidative stress and phospho-p38 expression. Oncol Lett 1159–1164. https://doi.org/10.3892/ol.2014.1863

Yasmin S, Mhlongo NN, Soliman ME et al. (2017) Comparative Design, In Silico Dockingand Predictive ADME/ TOX Properties of Some Novel 2, 4-hydroxy Derivatives of Thiazolidine-2, 4-diones as PPARγ Modulator. J Pharm Chem 4:11. https://doi.org/10.14805/jphchem.2017.art74

Zhao H, Chen G, Ye L, et al. (2018) DOK7V1 influences the malignant phenotype of lung cancer cells through PI3K/AKT/mTOR and FAK/paxillin signaling pathways. Int J Oncol 381–389. https://doi.org/10.3892/ijo.2018.4624